

II An Introduction to Plasma Turbulence

Now that we have visited most of the important neutral fluid turbulence topics, we can now re-examine some of the same concepts for plasmas. Since we are now going to couple the velocity field to E and B , things are obviously going to get messier in some ways, but it turns out that it also becomes simpler in others.

Recall that in hydro turbulence

- (I) Scale invariance and
- (II) Locality of energy transfer

$$\Rightarrow E \sim \frac{\delta u_e^2}{\tau_e} \sim \text{const.}$$

Further, there was only one time scale on the system, the eddy-turnover time

$$\tau_e \sim \frac{l}{\delta u_e} \Rightarrow E \sim \frac{\delta u_e^3}{l} \sim \text{const.} \therefore \delta u_e \sim (E l)^{1/3}$$

We had the Kolmogorov $4/5/3$ energy spectrum from simple dimensional analysis.

Now, let's look at the incompressible MHD eqns. We'll stick with the incompressible assumption because it makes things simpler, but it also turns out that Alfvén waves (which are incompressible) are the primary component of turbulence.

$$\rho_0(\partial_t \vec{u} + \vec{u} \cdot \nabla \vec{u}) = -\vec{\nabla} p + \vec{B} \cdot \frac{\nabla \vec{B}}{4\pi} + \nu \nabla^2 \vec{u} \quad (1)$$

$$\partial_t \vec{B} + \vec{u} \cdot \nabla \vec{B} = \vec{B} \cdot \nabla \vec{u} + \nu \frac{\nabla^2 \vec{B}}{\text{resistivity}} \quad (2)$$

where $p = p_0 + \frac{B^2}{8\pi}$ is the total pressure

If we assume we have a mean magnetic field, $\vec{B}_0 = B_0 \hat{z}$,

we immediately break the isotropy assumption of hydro

page 2 because, unlike a mean flow, a mean B_0 cannot be transformed away and introduces linear Alfvén waves. So, we now have an inherently anisotropic system w/ Alfvén waves (III)

Let's re-write eqns ① and ② in a more compact form by adding and subtracting them to obtain the Elsässer (1950) eqns

$$③ \partial_t \vec{z}^\pm + (\vec{v}_A \cdot \nabla) \vec{z}^\pm + (\vec{z}^\pm \cdot \nabla) \vec{z}^\pm = -\nabla \frac{P}{2} + \frac{\gamma+n}{2} \nabla^2 \vec{z}^\pm + \frac{\gamma-n}{2} \nabla^2 \vec{z}^\mp$$

where $\vec{z}^\pm = \vec{u} \pm \frac{\sqrt{B}}{4\pi P_0}$; $\vec{v}_A = v_A \hat{z}$; $\sqrt{B} = \vec{B} - \vec{B}_0$

A few important notes about these eqns

1) $\vec{z}^- = 0$ and $\vec{z}^+ = f(x, y, z + v_A t)$ or

$\vec{z}^+ = 0$ and $\vec{z}^- = f(x, y, z - v_A t)$

are exact solutions. They represent waves travelling down B_0 (\vec{z}^+) or up B_0 (\vec{z}^-)

2) The system supports two linear wave modes, both satisfying $\omega = k_n v_A^2$. These are the Alfvén waves with polarization in the $\hat{z} \times \hat{k}$ direction and $\hat{k} \times (\hat{z} \times \hat{k})$ for the pseudo-Alfvén waves, which are the incompressible limit of magnetosonic slow modes. Fast waves are ordered out of the system due to the incompressibility assumption, i.e., $c_s \rightarrow \infty$. It turns out that the slow modes are passive (will show this in a later lecture), so we will focus only on the Alfvén modes.

3) The system is closed. Taking the divergence of ③

$$\frac{1}{P_0} \nabla^2 P = -\nabla \cdot (\vec{z}^+ \cdot \nabla \vec{z}^+)$$

4) The nonlinear term, $\vec{z}^- \cdot \nabla \vec{z}^+$ requires oppositely propagating Alfvén waves. Further, if we just look at the

page 3 behavior of the dot product subject to the constraints above and Fourier transformation

$$ik^+ z^- z^+ [(\hat{z} \times \hat{k}^-) \cdot \hat{k}^+] (\hat{z} \times \hat{k}^+) = ik^+ z^- z^+ (\hat{z} \times \hat{k}^+) [\hat{z} \cdot (\hat{k}^- \times \hat{k}^+)]$$

So, the nonlinear term also requires that \vec{z}^+ and \vec{z}^- have non zero relative polarization.

Since we now know we are dealing with Alfvénic fluctuations, we know everything is in an Alfvénic state, $S_{\perp A} \sim \delta B_A$ scale-by-scale $\textcircled{IV} \Rightarrow$ some spectra for u and B . Given $\textcircled{I} \rightarrow \textcircled{IV}$, can we now construct the energy spectra for Alfvénic turbulence using here some dimensional arguments as $\textcircled{K41}$?

$$\epsilon_e \sim \frac{\delta u_e^2}{\tau_e} \sim \text{const} \quad \text{is still ok}$$

but we now have 2 choices for τ_e

$$\begin{aligned} &-\text{eddy turn over time} & \tau_{\text{eddy}} \sim \frac{\ell_1}{\delta u_e} & (\text{Nonlinear time}) \\ &-\text{Alfvén time} & \tau_A \sim \frac{\ell_1}{V_A} \end{aligned}$$

So, which one do we choose and why?

Iroshnikov (1964) - Kraichnan (1965) Theory

To derive an energy spectrum, IIC further assumed that the turbulence is weak:

The nonlinear term $|\vec{z}^\pm \cdot \nabla \vec{z}^\pm| \ll N_A \nabla_\parallel \vec{z}^\pm$ linear term \textcircled{II}

$$\text{This ratio } \frac{|\vec{z}^\pm \cdot \nabla \vec{z}^\pm|}{N_A \nabla_\parallel \vec{z}^\pm} \sim \frac{\vec{z}^\pm k_\perp}{V_A k_\parallel} \sim \frac{\delta u_\perp k_\perp}{V_A k_\parallel} = \frac{\tau_A}{\tau_{\text{eddy}}} =: \chi, \text{ the nonlinearity parameter}$$

$\chi \ll 1 \Rightarrow$ weak turbulence, linear term dominates

$\chi \gtrsim 1 \Rightarrow$ strong turbulence

This feature of turbulence was absent the hydro

systems we examined, but it exists when linear

page 4 terms come into play, e.g., Mach 3+1 flows, gravity waves, shallow water waves, etc.

When $\chi \ll 1$, each wave-wave interaction only decorrelates the wave a little. So,

Crossing / interaction time: $\Delta t \sim \frac{L}{V_A} \sim \tau_A$

Change in amplitude: $\delta t \Delta \delta u \sim \delta u \cdot \tau_A$

$$\Rightarrow \Delta \delta u_e \sim \frac{\delta u_e^2}{L_1} \Delta t \sim \delta u_e \frac{\delta u_e}{L_1} \frac{L_1}{V_A} \sim \delta u_e \chi$$

The "kicks" to the amplitude are random, so they add as

$$\sum_t \Delta \delta u_e \sim \delta u_e \chi \sqrt{N}, \text{ where } N = \frac{t}{\tau_A} \text{ is the \# of kicks}$$

the cascade time τ_e is defined as the time to achieve an order unity change in the amplitude

$$\text{So } \sum_t \Delta \delta u_e \sim \delta u_e \Rightarrow \tau_e \sim \tau_{\text{edd}}^2 / \tau_A$$

$$\therefore E \sim \frac{\delta u_e^2}{\tau_e} \sim \delta u_e^2 \frac{\delta u_e^2 L_{\perp}}{V_A L_{\perp}^2} \sim \text{const}$$

$$\Rightarrow \delta u_e \sim (E V_A)^{1/4} L_{\perp}^{1/2} L_{\parallel}^{-1/4}$$

It's also assumed that $L_{\parallel} \sim L_{\perp}$ (isotropy) (II)

$$\text{So, } (I) - (II) \Rightarrow \delta u_e \sim (E V_A)^{1/4} L^{1/4} \quad \text{or} \quad E \sim (E V_A)^{1/2} L^{-3/2}$$

Also, recall that we are dealing

with Alfvénic fluctuations, so $E_B \sim E_V$.

IK spectrum

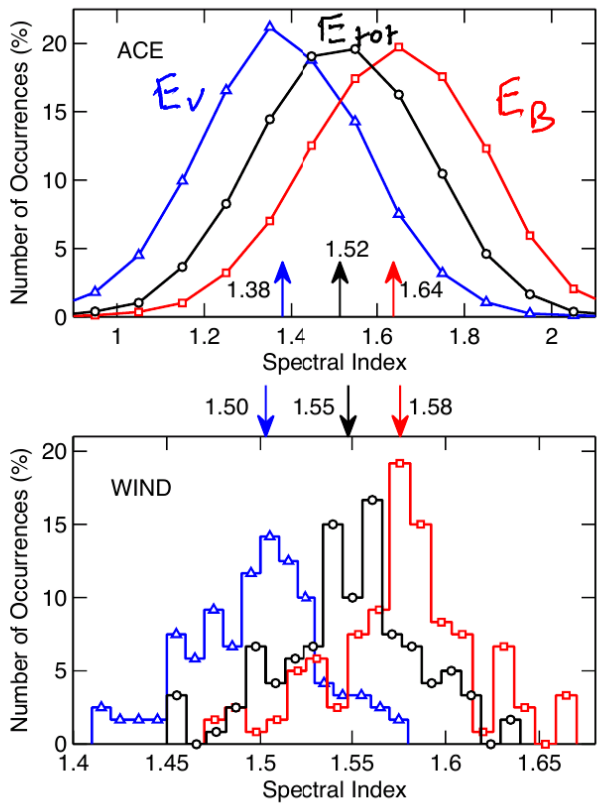
Is the weak interaction self-consistent, i.e., does it hold at all scales in the inertial range?

$$\chi \sim \frac{L}{V_A} \frac{\delta u_e}{L_{\perp}} \sim \frac{\delta u_e}{V_A} \sim \frac{(E V_A)^{1/4}}{V_A} L^{1/4}$$

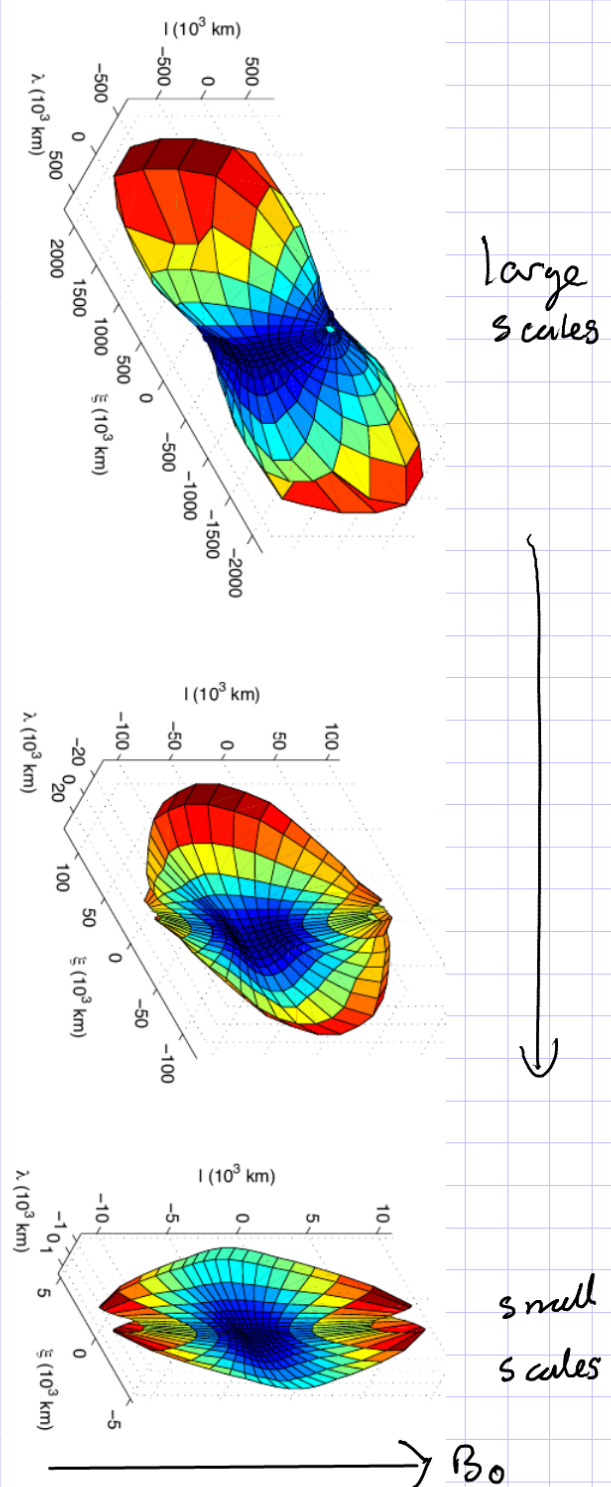
$$E \sim \frac{\delta u_L^2}{\tau_L} \sim \frac{\delta u_L^4}{V_A^2} \frac{1}{L} \Rightarrow \chi \sim \frac{\delta u_L}{V_A} \left(\frac{L}{L}\right)^{1/4}, \text{ which is}$$

small for $L \ll L$ provided $\delta u_L < V_A$, and it gets smaller with L

page 5 So, $I\kappa$ is self-consistent, and the community rejoiced... until high quality measurements became available. The observed spectra for the magnetic field are closer to $\kappa^{-5/3}$ than $\kappa^{-3/2}$ (1.666... and 1.5 are hard to differentiate). Also, DNSs showed that $l_1 \approx l_2$ is not satisfied.



From Boldyrev et al (2011)
 $ACE = 10$ yrs solar wind data
 $WIND = 11$ yrs " "



Surfaces of constant B
measured using ULysses
From Chen et al (2011)

page 6 Weak Turbulence (Montgomery & Turner 1981)

Let's see if we can fix IK based on data.

Consider the classic three wave interaction, 2 waves interact to produce a third.

We have two oppositely propagating Alfvén waves with $\omega = |k_n|v_A$. They must satisfy

$$\text{Energy: } \omega(\vec{k}_1) + \omega(\vec{k}_2) = \omega(\vec{k}_3) \Rightarrow k_{n_1} + k_{n_2} = k_{n_3}$$

$$\text{Momentum: } \vec{k}_1 + \vec{k}_2 = \vec{k}_3 \Rightarrow k_{n_1} - k_{n_2} = k_{n_3}$$

These can only be satisfied if $k_n = 0$, or $k_{n_2} = 0$, take $k_{n_2} = 0$

$\therefore k_{n_1} = k_{n_3}$. There is no parallel cascade! And, weak turbulence is mediated by $k_{n_1} = 0$ modes.

So, instead of \textcircled{VI} $l_{\perp} \sim l_n$, it should be \textcircled{VII} $l_n \sim L$

$$\text{and } \delta u_e \sim (E v_A)^{1/4} l_{\perp}^{1/2} l_n^{1/4} \sim \left(\frac{E v_A}{L}\right)^{1/4} l_{\perp}^{1/2} \quad \boxed{\Rightarrow E \sim \left(\frac{E v_A}{L}\right)^{1/2} k_{\perp}^{-2}}$$

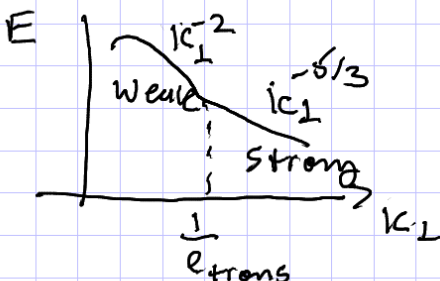
Now, under this new assumption.

Weak turb.
spectrum

$$X \sim \frac{\delta u_e}{v_A} \left(\frac{L}{l_{\perp}}\right)^{1/2}, \text{ which grows with decreasing } l_{\perp}!$$

$$X \sim 1 \text{ when } l_{\perp} \sim l_{\text{trans}} \sim L \left(\frac{\delta u_e}{v_A}\right)^2$$

So, at the transition scale, l_{trans} , the weak turbulence assumption breaks down and it becomes strong, $\tau_{\text{eddy}} \approx \tau_A$



So, let's explore strong turbulence

Let's replace our anisotropy assumption by something less restrictive.

Critical balance: $\chi \approx 1$ (VI), i.e., $\tau_A = \tau_{\text{edd}}$ or $|\vec{\zeta}^\pm| \approx |\vec{v}_A \nabla_\parallel \vec{\zeta}^\pm|$. So, $k_\perp \delta u_e \approx k_n v_A$

Now, there is just one time scale $\tau_e \approx l_\perp / \delta u_e$

$$\therefore E \sim \frac{\delta u_e^2}{\tau_e} \sim \frac{\delta u_e^3}{l_\perp} \Rightarrow \delta u_e \sim (E l_\perp)^{1/3} \Rightarrow E \sim E^{2/3} k_\perp^{-5/3}$$

GS spectrum

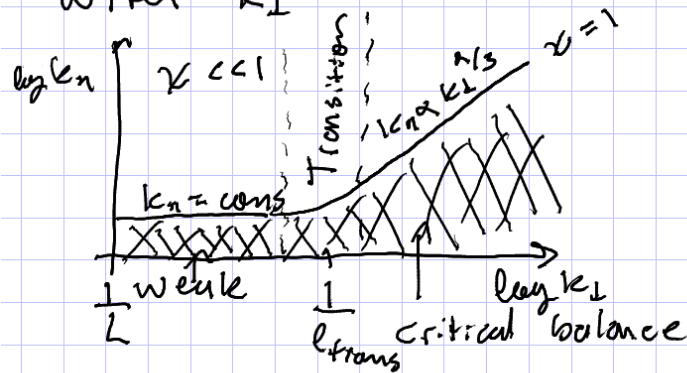
Together with $\chi \approx 1$

$$k_n v_A \sim k_\perp \delta u_e \sim E^{1/3} k_\perp^{2/3} \Rightarrow k_\parallel \sim \frac{E^{1/3}}{V_A} k_\perp^{2/3}$$

reduced parallel cascade

So, GS predict that the wave vector anisotropy grows

with k_\perp



Since there is now a parallel cascade, we can also derive a parallel wave number spectrum

$$E \sim \frac{\delta u_e^2}{\tau_e} \sim \delta u_e^2 V_A k_n \Rightarrow \delta u_e^2 \sim (E/V_A) k_n^{-1/2}$$

$$\Rightarrow E(k_n) \sim \frac{E}{V_A} k_n^{-1/2}$$

End of the inertial range (assuming l_\parallel or l_\perp > kinetic scales)

We now have both viscosity and resistivity that could terminate our inertial range. So, we can construct two Reynolds type numbers

As in hydro $Re := \frac{\text{convection}}{\text{viscous}} = \frac{\delta u_L L}{\nu}$

Similarly, the magnetic Reynolds number is

$Re_m = \frac{\text{convection}}{\text{resistive}} = \frac{\delta u_L L}{\eta}$, this should not be confused with the Lundquist number $S := \frac{L V_A}{\eta}$, which relates the Alfvén crossing time and resistive diffusion.

The magnetic Prandtl number is the ratio of

$Pr_m = \frac{Re_m}{Re} = \frac{\eta}{\nu}$ and characterizes the relative strength of viscous to magnetic diffusivity.

For simplicity, we'll assume $Pr_m \gg 1$.

So, at the viscous scale

$$\epsilon \sim \frac{\delta u_{Lx}^3}{l_{2D}} \sim \nu \frac{\delta u_{Lx}^2}{l_{2D}^2} \quad \text{and} \quad \delta u_{Lx}^2 \sim (\epsilon l_{2D})^{2/3}$$

$$\Rightarrow l_{2D} \sim \frac{\nu^{3/4}}{\epsilon^{1/4}} \quad \text{as before}$$

weak turbulence result
see \star

$$\text{but } \nu^{3/4} = Re^{-3/4} \delta u_L^{3/4} L^{3/4} \quad \text{and} \quad \epsilon^{1/4} \sim \frac{\delta u_L}{(V_A L)^{1/4}}$$

$$\Rightarrow l_{2D} \sim Re^{-3/4} L \underbrace{\left(\frac{V_A}{\delta u_L}\right)^{1/4}}_{\text{new}}$$

When is $l_{trans} \gg l_1 \gg l_{2D}$ valid?

$$l_{trans} \sim L \left(\frac{\delta u_L}{V_A}\right)^2 \gg l_{2D} \sim Re^{-3/4} L \left(\frac{V_A}{\delta u_L}\right)^{1/4}$$

So, $Re \gg (V_A / \delta u_L)^3$ to have strong turbulence and

$\Rightarrow \frac{\delta u_L}{V_A}$ must be true for weak turbulence

References

- 1) W. M. Eissner Phys Rev 79, 1 (1950).
- 2) R. S. Iroshnikov Sov. Astron 7, 566 (1964) [English translation]
- 3) R. H. Kraichnan Phys. Fluids 9, 1385 (1965)
- 4) S. Boldyrev et al ApJL 741, 1 (2011)
- 5) C. Chen et al ApJ 758, 2 (2012)
- 6) D. Montgomery & L. Turner Phys Fluids 24, 885 (1981)
- 7) P. Goldreich & S. Sridhar ApJ 438, 763 (1995)

III Intro. (continued) & Weak Turbulence

Last time I introduced most of the important concepts in incompressible plasma turbulence. One concept I stressed was that Alfvénic turbulence, i.e AW-AW collisions, requires relatively polarized, oppositely propagating Alfvén waves. This necessarily implies the Alfvénic turbulence only works in 3D. The guide field direction is necessary for AW propagation, i.e., $\mathbf{v}_A \cdot \vec{\mathbf{z}}^\pm$ is only non-zero when $\nabla_{||} \vec{\mathbf{z}}^\pm \neq 0$. Since the AWs must be relatively polarized for $\vec{\mathbf{z}}^\pm \cdot \vec{\mathbf{z}}^\pm$ to be nonzero, both directions perpendicular to \mathbf{B}_0 are needed. So, -2D simulations w/ \mathbf{B}_0 out of the plane retain the NL term but lack linear AWs. Note that in this limit, weak turbulence is no longer applicable and the Elsässer equations very closely resemble the Navier-Stokes eqns.

-2D simulations w/ \mathbf{B}_0 in the plane (fully or partially) permit the propagation of AWs but AW-AW nonlinear term vanishes.

What about other combinations of interacting modes, pseudo Alfvén wave-Alfvén wave, PW-PW, and AW-PW? To do this, let's look at the NL term in more detail. First, let's specify for a wave w/ wave vector \vec{k} and orthonormal basis $(\hat{\mathbf{z}}, \hat{\mathbf{k}}_\perp, \hat{\mathbf{z}} \times \hat{\mathbf{k}}_\perp)$. Then an AW polarized in $\hat{\mathbf{z}} \times \hat{\mathbf{k}}$ direction becomes $\hat{\mathbf{z}} \times \hat{\mathbf{k}}_S$. the PW polarized in $\hat{\mathbf{k}} \times (\hat{\mathbf{z}} \times \hat{\mathbf{k}})$ $\rightarrow -\frac{k_n}{k^2} \hat{\mathbf{k}}_\perp + \frac{k_n}{k^2} \hat{\mathbf{z}}$. Now consider any $\vec{\mathbf{z}}^\pm = k_S^\pm - k_n^\pm \hat{\mathbf{z}}$ cascaded first by an AW

AW-AW and AW-PW

$$\vec{\mathbf{z}}_A \cdot \nabla \vec{\mathbf{z}}^\pm \propto \hat{\mathbf{z}} \cdot (\hat{\mathbf{k}}_S^\pm \times \hat{\mathbf{k}}_\perp^\pm)$$

page 2 In both the AW-AW and PW-PW regime the waves be relatively polarized, i.e., both perpendicular directions are required

PW-AW and PW-PW

$$\vec{z}_P \cdot \nabla \vec{z}^+ \propto -k_1^+ \frac{k_{\perp P}}{k_P} (\hat{k}_{\perp P} \cdot \hat{k}_1^+) - k_{11}^- \frac{k_{\perp P}}{k_P}$$

This NL interaction requires parallel variation. In the limit that $k_n \ll k_1$, as we showed happens in weak & strong turbulence, this term tends to zero. However, in 2D w/ the guide field on the plane, this becomes the sole NL term.

- In 3D, AW are the primary constituent of turbulence.
- In 2D w/ B_0 on the plane, PW are the primary constituent.
- In 2D w/ B_0 out of the plane, neither wave mode exists and the turbulence is neutral fluid like.

Energy Conservation of AW collisions

Conserv the \vec{z}^+ equation dotted w/ \vec{z}^+

$$\frac{\partial}{\partial t} \left(\frac{\vec{z}^{+2}}{2} \right) = \vec{z}^+ \cdot (\vec{v}_A \cdot \nabla \vec{z}^-) - \vec{z}^+ \cdot (\vec{z}^- \cdot \nabla \vec{z}^+) - \vec{z}^+ \cdot \nabla P$$

Taking advantage of $\nabla \cdot \vec{z}^\pm = 0$ and re-arranging \Rightarrow

$$\frac{\partial}{\partial t} \left(\frac{\vec{z}^{+2}}{2} \right) = \nabla \cdot [(\vec{v}_A - \vec{z}^-) \frac{\vec{z}^{+2}}{2}] - \nabla \cdot (P \vec{z}^+)$$

Integrating over all space and using the divergence theorem

$$\partial_t \int d\vec{r} \frac{\vec{z}^{+2}}{2} = \oint d\vec{S} \cdot [(\vec{v}_A - \vec{z}^-) \frac{\vec{z}^{+2}}{2}] - \oint d\vec{s} \cdot (\vec{z}^+ P)$$

The RHS vanishes for, e.g., periodic boundary conditions.

$$\text{So, } \partial_t \int d\vec{r} \frac{\vec{z}^{+2}}{2} = 0. \text{ Similarly, } \partial_t \int d\vec{r} \frac{\vec{z}^{-2}}{2} = 0.$$

\therefore the energy of + (-) wave packets is not changed by NL interactions w/ - (+) packets. In other words, the collisions are elastic.

Now let's examine weak turbulence in its full perturbative glory. We want to solve

$$\partial_t \tilde{\zeta}^\pm + v_A \cdot \nabla \tilde{\zeta}^\pm = - \tilde{\zeta}^\mp \cdot \nabla \tilde{\zeta}^\pm - \nabla P, \quad \nabla \cdot \tilde{\zeta}^\pm = 0$$

order by order. First, the ∇P term makes asymptotic solutions difficult. So, let's take the curl of the Elsasser eqns to eliminate it. Also, we'll re-write the equations in terms of the Elsasser potentials, where $\xi^\pm = \tilde{\zeta}^\pm \Psi$ and

$$\tilde{u}_\perp = \hat{\zeta} \times \vec{\nabla}_\perp \Psi \text{ and } \frac{\tilde{B}_\perp}{B_0} = \hat{\zeta} \times \vec{\nabla}_\perp \Psi$$

$$\text{so } \frac{\tilde{u}_\perp}{v_A} = \hat{\zeta} \times \vec{\nabla}_\perp \frac{1}{2v_A} (\xi^+ + \xi^-)$$

$$\text{and } \frac{\tilde{B}_\perp}{B_0} = \hat{\zeta} \times \vec{\nabla}_\perp \frac{1}{2v_A} (\xi^+ - \xi^-)$$

So, we now have

$$\partial_t \nabla_\perp^2 \xi^\pm + v_A \partial_z \nabla_\perp^2 \xi^\pm = -\frac{1}{2} [\{ \xi^+, \nabla_\perp^2 \xi^- \} + \{ \xi^-, \nabla_\perp^2 \xi^+ \} - \nabla_\perp^2 \{ \xi^+, \xi^- \}]$$

where the Poisson brackets are defined as $\{ f, g \} = \hat{\zeta} \cdot (\vec{\nabla}_\perp f \times \vec{\nabla}_\perp g)$

We begin with two counter-propagating AUs

$$\tilde{\zeta}_+^\pm = \zeta_+ w_0 (k_{\perp x} x - k_{\perp z} z - w_0 t) \hat{y} = \frac{\zeta_\pm}{2} [e^{i(k_{\perp x} x - k_{\perp z} z - w_0 t)} + e^{-i(k_{\perp x} x - k_{\perp z} z - w_0 t)}] \hat{y}$$

$$\tilde{\zeta}_-^\pm = \zeta_- w_0 (k_{\perp y} y + k_{\perp z} z - w_0 t) \hat{x} = \frac{\zeta_\pm}{2} [e^{i(k_{\perp y} y + k_{\perp z} z - w_0 t)} + e^{-i(k_{\perp y} y + k_{\perp z} z - w_0 t)}] \hat{x}$$

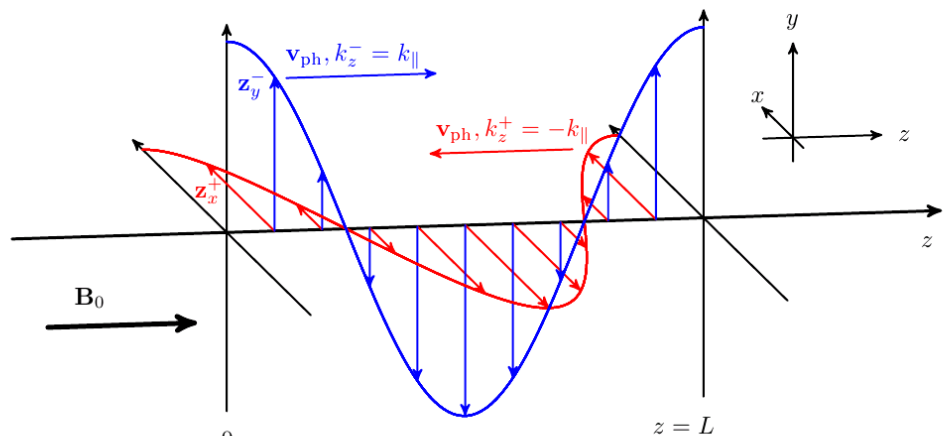
$$\text{or } \xi_+^+ = \frac{\zeta_+}{2ik_1} [e^{i(k_{\perp x} x - k_{\perp z} z - w_0 t)} - CC]$$

$$\xi_+^- = \frac{\zeta_-}{2ik_1} [e^{i(k_{\perp y} y + k_{\perp z} z - w_0 t)} - CC]$$

Schematic of the

initial conditions

from Howes (2013).



page 4 To simplify our problem, we'll take advantage of the method of characteristics to simplify the linear terms. Let

$$e_{\pm} \approx z \pm v_A t \Rightarrow z = \frac{1}{2}(e_+ + e_-) \text{ and } t = \frac{1}{2v_A}(e_+ - e_-)$$

$$\text{Then } \partial_t \nabla_L^2 g^{\pm} = v_A \partial_z \nabla_L^2 g^{\pm} = T2v_A \frac{\partial \nabla_L^2 g^{\pm}}{\partial e_{\mp}},$$

so we now have

$$\frac{\partial \nabla_L^2 g^{\pm}}{\partial e_{\mp}} = \pm \frac{1}{4v_A} \left[\{g^+, \nabla_L^2 g^- \} + \{g^-, \nabla_L^2 g^+ \} \right]$$

and our initial condition becomes

$$g_1^+ = \frac{z_+}{2ik_1} [e^{i(k_1 x - k_n e_+)} - CC]$$

$$g_1^- = -\frac{z_-}{2ik_1} [e^{i(k_1 y + k_n e_-)} - CC]$$

Now, we can consider an asymptotic expansion in terms of

$$\frac{z_{\pm}}{v_A} \sim \epsilon \ll 1 \quad (\text{weak turbulence})$$

$$\text{So, } g^{\pm} \approx g_0^{\pm} + \epsilon g_1^{\pm} + \epsilon^2 g_2^{\pm} + \dots \quad \text{and } g_n^{\pm}(t=0) = 0 \text{ for } n > 1$$

We also assume that $\overset{\circ}{g}_0^{\pm} = O(\epsilon)$, $O(1)$ trivially gives $O = 0$

$\mathcal{O}(\epsilon)$ only the linear term survives and

$$\frac{\partial \nabla_L^2 g_1^{\pm}}{\partial e_{\mp}} = 0, \text{ which our initial condition trivially satisfies}$$

$\mathcal{O}(\epsilon^2)$

$$\frac{\partial \nabla_L^2 g_2^{\pm}}{\partial e_{\mp}} = \pm \frac{1}{4v_A} \left[\{g_1^+, \nabla_L^2 g_1^- \} + \{g_1^-, \nabla_L^2 g_1^+ \} \right] \quad \text{①}$$

②

③

Inserting our $\mathcal{O}(\epsilon)$ solution, terms ① and ② cancel. So, the NL contribution is due solely to term ③, and we can rewrite the eqn as

$$\frac{\partial \nabla_L^2 g_2^{\pm}}{\partial e_{\mp}} = -k_1^2 z_+ z_- \left\{ \cos[k_1 x + k_1 y - k_n(e_+ - e_-)] + \cos[k_1 x - k_1 y - k_n(e_+ + e_-)] \right\}$$

Solving this set of equations is relatively straightforward, but we need to be a little careful w/ the limits of integration

page 4 We want to integrate from $t'=0$ to $t'=t$, but $t'=0$

page 5 corresponds to $\varphi_+ = \varphi_-$. So we need the following integrals

$$\int_{\varphi_+}^{\varphi_-} \frac{\partial \nabla_L^2 \xi_2^+}{\partial \varphi'_-} d\varphi'_- = \nabla_L^2 \xi_2^+(x, y, \varphi_+, \varphi_-) - \nabla_L^2 \xi_2^+(x, y, \varphi_-, \varphi_-) = 0$$

$$= \nabla_L^2 \xi_2^+(x, y, \varphi_+, \varphi_-)$$

$\xi_2^+(x, y, \varphi_+, \varphi_-) = 0$ because $\xi_2^+(t=0) = 0$. Integrating out the ∇_L^2 is trivial, and the end result when converted back to z and t

$$\xi_2^+ = \frac{z_+ z_-}{8w_0} \left\{ \sin[k_1 x + k_2 y - 2w_0 t] - \sin[k_1 x + k_2 y] - \sin[k_1 x - k_2 y - 2k_n z] + \sin[k_1 x - k_2 y - 2k_n z - 2w_0 t] \right\}$$

$$\xi_2^- = -\frac{z_+ z_-}{8w_0} \left\{ \sin[k_1 x + k_2 y - 2w_0 t] - \sin[k_1 x + k_2 y] + \sin[k_1 x - k_2 y - 2k_n z] - \sin[k_1 x - k_2 y - 2k_n z + 2w_0 t] \right\}$$

or more instructively

$$\frac{\tilde{B}_{12}}{B_0} = \frac{z_+ z_-}{16V_A^2} \frac{k_L}{k_n} \left\{ [2 \cos(k_1 x + k_2 y - 2w_0 t) - 2 \cos(k_1 x + k_2 y)] (\hat{x} + \hat{y}) + [\cos(-k_1 x + k_2 y + 2k_n z + 2w_0 t) - \cos(-k_1 x + k_2 y + 2k_n z - 2w_0 t)] (\hat{x} + \hat{y}) \right\}$$

$$\frac{\tilde{G}_{12}}{V_A} = -\frac{z_+ z_-}{16V_A^2} \frac{k_L}{k_n} \left\{ [2 \cos(-k_1 x + k_2 y + 2k_n z) - \cos(-k_1 x + k_2 y + 2k_n z + 2w_0 t)] (\hat{x} + \hat{y}) - \cos(-k_1 x + k_2 y + 2k_n z - 2w_0 t)] (\hat{x} + \hat{y}) \right\}$$

where $w_0 = k_n V_A$. What does all of this mean physically?

Well, at $\Theta(\epsilon)$ we had two Fourier components:

$$\left(\frac{k_x}{k_L}, \frac{k_y}{k_L}, \frac{k_z}{k_n} \right) = (1, 0, -1) \text{ and } (0, 1, 1), \text{ which were oppositely}$$

propagating AWs. At $\Theta(\epsilon^2)$ we again have two Fourier modes $(1, 1, 0)$ and $(-1, 1, 2)$. The $(-1, 1, 2)$ mode corresponds to two counter propagating linear AWs with $\omega = \pm k_z V_A = \pm 2k_n V_A$.

These modes have the same polarization $(\hat{x} + \hat{y})$ and only linearly superpose to form a standing wave. The $(1, 1, 0)$ is purely magnetic and is a NL fluctuation (the $k_n = 0$ mode) that oscillates with frequency $2w_0$ — it does not gain energy as time progresses. This $k_n = 0$ mode corresponds to a shear in the total magnetic field across the perpendicular plane. Term ⑨ exists to satisfy $\xi_2^+(t=0) = 0$.

So, the 3-wave interaction has not produced a secular cascade of energy to smaller scales. Let's continue to $\mathcal{O}(\epsilon^3)$

$$\frac{\partial \nabla_1^2 \zeta_3^\pm}{\partial \varphi_2^\pm} = \pm \frac{1}{4v_A} \left[\left\{ \zeta_1^\pm, \nabla_1^2 \zeta_2^\mp \right\} + \left\{ \zeta_2^\pm, \nabla_2^2 \zeta_1^\mp \right\} + \left\{ \zeta_1^\mp, \nabla_2^2 \zeta_2^\pm \right\} + \right. \\ \left. \left\{ \zeta_2^\mp, \nabla_1^2 \zeta_1^\pm \right\} + \nabla_1^2 \left\{ \zeta_1^\pm, \zeta_2^\pm \right\} \mp \nabla_2^2 \left\{ \zeta_1^\pm, \zeta_2^\mp \right\} \right]$$

Much algebra later yields (copied from Howes (2013))

$$\frac{\mathbf{B}_{\perp 3}}{B_0} = \frac{z_+^2 z_-}{640 v_A^3 k_{\parallel}^2} \left\{ \begin{aligned} & [-8\omega_0 t \sin(2k_{\perp}x + k_{\perp}y - k_{\parallel}z - \omega_0 t) + 3 \cos(2k_{\perp}x + k_{\perp}y - k_{\parallel}z + \omega_0 t) \\ & - 10 \cos(2k_{\perp}x + k_{\perp}y - k_{\parallel}z - \omega_0 t) + 7 \cos(2k_{\perp}x + k_{\perp}y - k_{\parallel}z - 3\omega_0 t)] (-\hat{x} + 2\hat{y}) \\ & + [-2 \cos(-2k_{\perp}x + k_{\perp}y + 3k_{\parallel}z + 3\omega_0 t) + \cos(-2k_{\perp}x + k_{\perp}y + 3k_{\parallel}z + \omega_0 t) \\ & + 4 \cos(-2k_{\perp}x + k_{\perp}y + 3k_{\parallel}z - \omega_0 t) - 3 \cos(-2k_{\perp}x + k_{\perp}y + 3k_{\parallel}z - 3\omega_0 t)] (\hat{x} + 2\hat{y}) \\ & + [-10 \cos(k_{\perp}y + k_{\parallel}z + \omega_0 t) + 20 \cos(k_{\perp}y + k_{\parallel}z - \omega_0 t) - 10 \cos(k_{\perp}y + k_{\parallel}z - 3\omega_0 t)] \hat{x} \} \\ & + \frac{z_+ z_-^2}{640 v_A^3 k_{\parallel}^2} \left\{ \begin{aligned} & [8\omega_0 t \sin(k_{\perp}x + 2k_{\perp}y + k_{\parallel}z - \omega_0 t) + 3 \cos(k_{\perp}x + 2k_{\perp}y + k_{\parallel}z + \omega_0 t) \\ & - 2 \cos(k_{\perp}x + 2k_{\perp}y + k_{\parallel}z - \omega_0 t) - \cos(k_{\perp}x + 2k_{\perp}y + k_{\parallel}z - 3\omega_0 t)] (-2\hat{x} + \hat{y}) \\ & + [3 \cos(-k_{\perp}x + 2k_{\perp}y + 3k_{\parallel}z + 3\omega_0 t) - 4 \cos(-k_{\perp}x + 2k_{\perp}y + 3k_{\parallel}z + \omega_0 t) \\ & - \cos(-k_{\perp}x + 2k_{\perp}y + 3k_{\parallel}z - \omega_0 t) + 2 \cos(-k_{\perp}x + 2k_{\perp}y + 3k_{\parallel}z - 3\omega_0 t)] (2\hat{x} + \hat{y}) \\ & + [10 \cos(k_{\perp}x - k_{\parallel}z + \omega_0 t) - 20 \cos(k_{\perp}x - k_{\parallel}z - \omega_0 t) + 10 \cos(k_{\perp}x - k_{\parallel}z - 3\omega_0 t)] \hat{y} \} \end{aligned} \right. \end{aligned} \right. \quad (40)$$

$$\frac{c\mathbf{E}_{\perp 3}}{v_A B_0} = \frac{z_+^2 z_-}{640 v_A^3 k_{\parallel}^2} \left\{ \begin{aligned} & [8\omega_0 t \sin(2k_{\perp}x + k_{\perp}y - k_{\parallel}z - \omega_0 t) + 3 \cos(2k_{\perp}x + k_{\perp}y - k_{\parallel}z + \omega_0 t) \\ & - 2 \cos(2k_{\perp}x + k_{\perp}y - k_{\parallel}z - \omega_0 t) - \cos(2k_{\perp}x + k_{\perp}y - k_{\parallel}z - 3\omega_0 t)] (2\hat{x} + \hat{y}) \\ & + [-2 \cos(-2k_{\perp}x + k_{\perp}y + 3k_{\parallel}z + 3\omega_0 t) + 7 \cos(-2k_{\perp}x + k_{\perp}y + 3k_{\parallel}z + \omega_0 t) \\ & - 8 \cos(-2k_{\perp}x + k_{\perp}y + 3k_{\parallel}z - \omega_0 t) + 3 \cos(-2k_{\perp}x + k_{\perp}y + 3k_{\parallel}z - 3\omega_0 t)] (-2\hat{x} + \hat{y}) \\ & + [10 \cos(k_{\perp}y + k_{\parallel}z + \omega_0 t) - 20 \cos(k_{\perp}y + k_{\parallel}z - \omega_0 t) + 10 \cos(k_{\perp}y + k_{\parallel}z - 3\omega_0 t)] \hat{y} \} \\ & + \frac{z_+ z_-^2}{640 v_A^3 k_{\parallel}^2} \left\{ \begin{aligned} & [8\omega_0 t \sin(k_{\perp}x + 2k_{\perp}y + k_{\parallel}z - \omega_0 t) - 3 \cos(k_{\perp}x + 2k_{\perp}y + k_{\parallel}z + \omega_0 t) \\ & + 10 \cos(k_{\perp}x + 2k_{\perp}y + k_{\parallel}z - \omega_0 t) - 7 \cos(k_{\perp}x + 2k_{\perp}y + k_{\parallel}z - 3\omega_0 t)] (\hat{x} + 2\hat{y}) \\ & + [3 \cos(-k_{\perp}x + 2k_{\perp}y + 3k_{\parallel}z + 3\omega_0 t) - 8 \cos(-k_{\perp}x + 2k_{\perp}y + 3k_{\parallel}z + \omega_0 t) \\ & + 7 \cos(-k_{\perp}x + 2k_{\perp}y + 3k_{\parallel}z - \omega_0 t) - 2 \cos(-k_{\perp}x + 2k_{\perp}y + 3k_{\parallel}z - 3\omega_0 t)] (-\hat{x} + 2\hat{y}) \\ & + [-10 \cos(k_{\perp}x - k_{\parallel}z + \omega_0 t) + 20 \cos(k_{\perp}x - k_{\parallel}z - \omega_0 t) - 10 \cos(k_{\perp}x - k_{\parallel}z - 3\omega_0 t)] \hat{x} \} \end{aligned} \right. \end{aligned} \right. \quad (41)$$

where $\frac{\tilde{\zeta}_{13}}{v_A} = \frac{c}{v_A B_0} (\tilde{\mathbf{E}}_{13} \times \hat{z})$. Now, we have secularly growing terms (those proportional to t)! these correspond to AWs with mode numbers $(2, 1, -1)$ and $(1, 2, 1)$, frequencies $\omega = \mp k_{\parallel} v_A$, and oppositely propagating along B_0 . These modes have the same parallel wave number as the initial AWs but a larger perpendicular wave number, $\sqrt{5} k_{\perp}$ compared to k_{\perp} . These are the fundamental

page 7 NL interactions for our initial conditions. The remaining modes correspond to four oscillating linear AWs with mode numbers $(2, 1, -1)$, $(1, 2, 1)$, $(-1, 2, 3)$, and $(-2, 1, 3)$ and 2 AWs with $(1, 0, -1)$ and $(0, 1, 1)$. The latter two dampen the amplitude of the $\mathcal{O}(\epsilon)$ solution, and the former four all have $k_1' = \sqrt{5} k_1$. Schematically, the transfer of energy looks like the following.

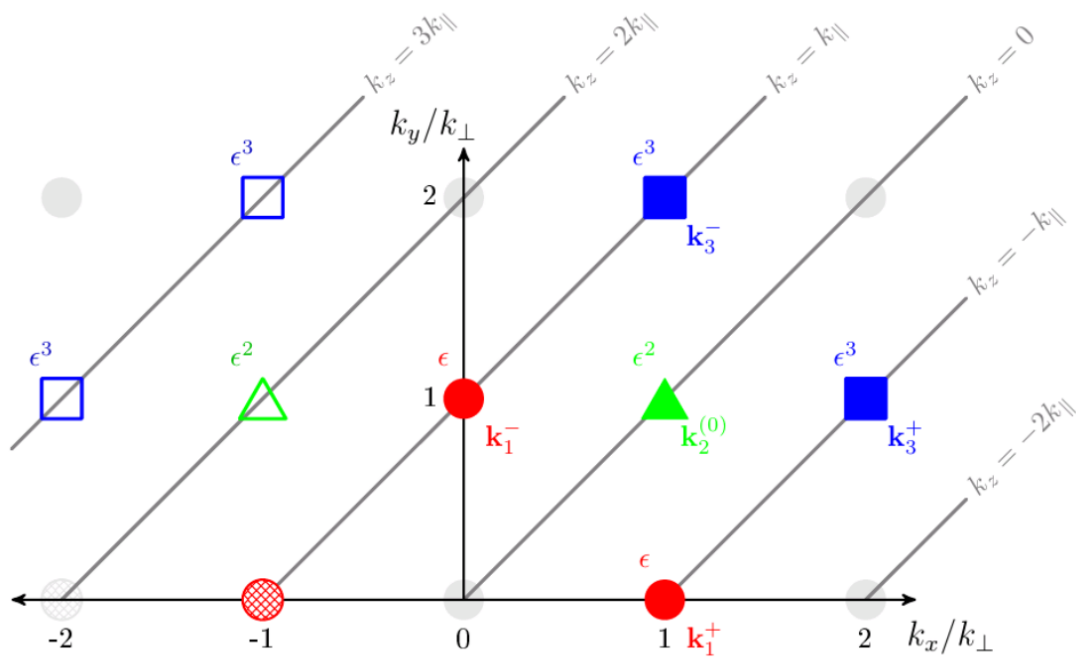
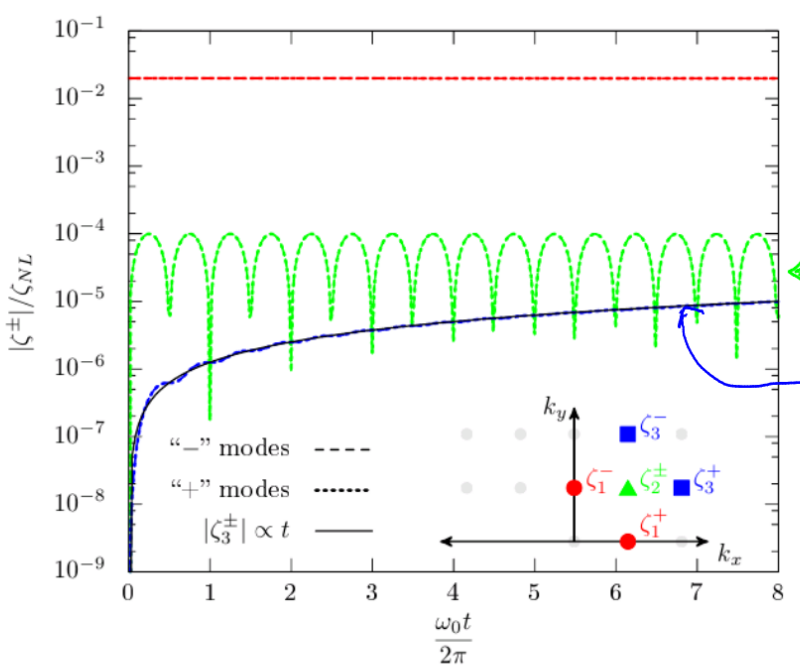


FIG. 2. Schematic diagram of the Fourier modes in the (k_x, k_y) perpendicular plane arising in the asymptotic solution. The Fourier modes depicted are the primary $\mathcal{O}(\epsilon)$ modes (circles), secondary $\mathcal{O}(\epsilon^2)$ modes (triangles), and tertiary $\mathcal{O}(\epsilon^3)$ modes (squares). Filled symbols denote the key Fourier modes that play a role in the secular transfer of energy to small scales in the Alfvén wave collision. The parallel wavenumber k_z for each of the modes is indicated by the diagonal grey lines, a consequence of the resonance conditions for the wavevector.

Note that independent conservation of ϵ^+ and ϵ^- energies and the lack of a parallel cascade means that the cascade to higher k_z occurs along diagonal lines, grey lines of fixed k_z on the figure.

To see the energy evolution of the important modes for the NL evolution, we turn to a DNS using gyrokinetics



From Nielsen et al (2013)

Oscillatory $\Theta(\epsilon^2)$
 $k_n=0$ mode

Secularly growing
 $\Theta(\epsilon^3)$ modes

FIG. 2. Evolution of the normalized amplitude $|\zeta^\pm|/\zeta_{NL}$ of the key Fourier modes vs. time $\omega_0 t/2\pi$ over eight periods of the primary Alfvén waves. The color map is the same as Figure 1, and a linear increase with time is indicated by the solid black line.

3-wave vs 4-wave

At $\Theta(\epsilon^2)$ we found that $\omega_{1+} + \omega_{1-} \approx \omega_{20}$, where ω_{20} corresponds to the $k_n=0$ mode, which does not grow with time. At $\Theta(\epsilon^3)$ we had another 3 wave interaction, $\omega_{1+} + \omega_{20} = \omega_{3+}$. But, this is really a 4-wave interaction $\omega_{1+} + \omega_{20} = \omega_{1+} + \omega_{1-} + \omega_{1+} + \omega_{1-} = \omega_{3+}$. So, 4-wave interactions are actually at the heart of the weak NL energy cascade. Note that the $\Theta(\epsilon^3)$ 4-wave interaction still satisfies the 3-wave requirements; two modes interact through a $k_n=0$ mode, which corresponds to field line wander.

References

- 1) G. G. Howes & K. D. Nielsen Phys Plasmas 20, 7 (2013)
 - 2) K. D. Nielsen & G. G. Howes, B. W. Dobrowol Phys Plasmas 20, 7 (2013)
 - 3) D. J. Drake et al Phys Plasmas 20, 7 (2013)
 - 4) N. Tronko, S. V. Nazarenko, & S. Balcerow Phys Rev E 87, 3 (2013)
 - 5) G. G. Howes arXiv 1306.4589 (2013)
- 1-3 cover weak turbulence in great detail theoretically (1), numerically (2), and experimentally (3). (4&5) discussed weak turbulence in 2 vs 3D.

page 1 Strong Turbulence I: the Controversy of the GS Model

last time we focused on weak turbulence, which we have shown increases in strength as the cascade proceeds to smaller scales. When $\chi \ll 1$ is no longer satisfied, the perturbative solution we derived breaks down and all orders begin to contribute equally. At that point, the perturbative approach becomes useless, and we are back to trying to "solve" turbulence in the same sense we solved it in neutral fluids, e.g., through a closure model and exact relationships of 3rd order structure functions. But, that approach is even worse and less accurate in plasmas. We'll discuss that in a later lecture. For now, let's focus on what we can learn from simpler concepts in strong turbulence.

3D Spectrum of GS turbulence (GS = Goldreich-Sridhar)

Previously, I demonstrated the critical balance assumption, $\chi \approx 1$, leads to different perpendicular and parallel 1D spectra $E(k_\perp) \sim \epsilon^{2/3} k_\perp^{-5/3}$ and $E(k_n) \sim \frac{\epsilon}{v_A} k_n^{-2}$. These can be combined into a 3D spectrum, where $E = \int d\vec{k} E(k_\perp, k_n)$.

GS 95 assumed it to be of the form $E(k_\perp, k_n) \sim \frac{v_A^2}{L^{1/3}} k_\perp^{-10/3} f(k_n k_\perp^{-2/3} L^{1/3})$, where $f(u) > 1$ is symmetric, $f(|u| > 1) \ll 1$ and $\int_{-\infty}^{\infty} du f(u) \approx 1$. Later, MG 01 altered it slightly so that $f(|u| \leq 1) \approx 1$. The argument for the shape of $f(|u| \leq 1) \approx 1$ follows from fluctuations with scale k_1^{-1} being independent: $f(k_1) \approx k_1^{2/3} L^{-1/3}$. In other words, such fluctuations are equivalent to uncorrelated

page 2 (White) noise. How does one see this physically? The natural timescale at which information is propagated incompressible in an ^v plasma is the Alfvén time, $\tau_A \approx \frac{1}{k_n v_A}$. Critical balance is the statement that $\tau_A \approx \tau_{\text{Eddy}} \approx \frac{1}{k_n v_L}$. If at scale k_\perp^1 , eddies in two planes ^{are} separated by a distance greater than given by critical balance, $l_{\parallel 1} \gtrsim l_\perp \frac{v_A}{\delta v_L}$, information does not have time to propagate between the planes before a full τ_{Eddy} is completed. Therefore, when $k_n \lesssim k_\perp^{2/3} L^{-1/3}$ planes are uncorrelated because $\delta v_L \sim l_\perp^{1/3}$. Note that these uncorrelated fluctuations have $\chi > 1$. So, schematically

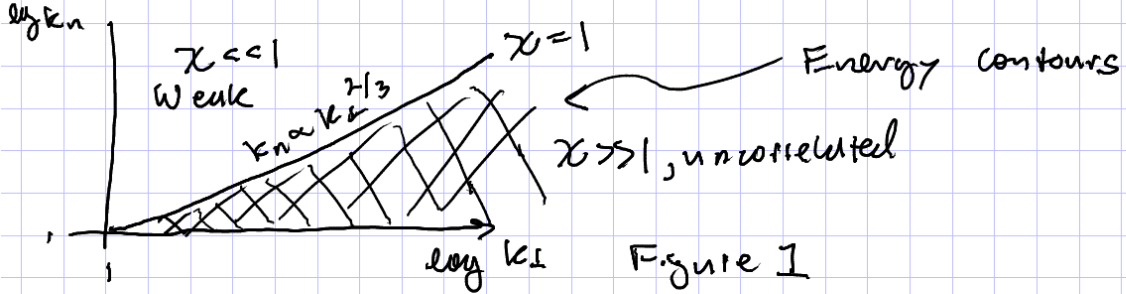
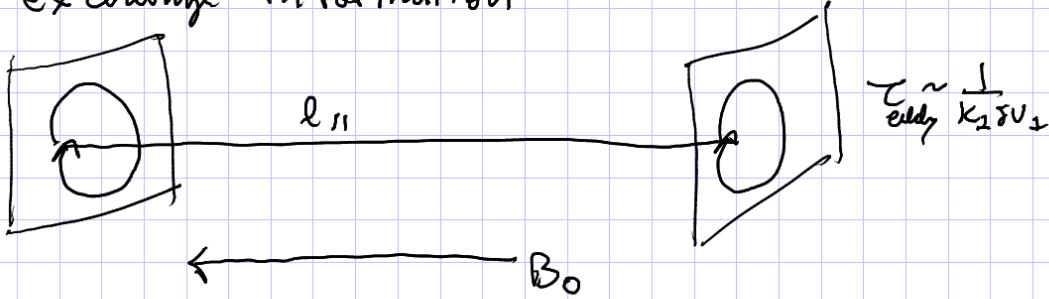


Figure 1

But what happens to these uncorrelated fluctuations? Well, the only way fluctuations can remain 2D like is if they can exchange information

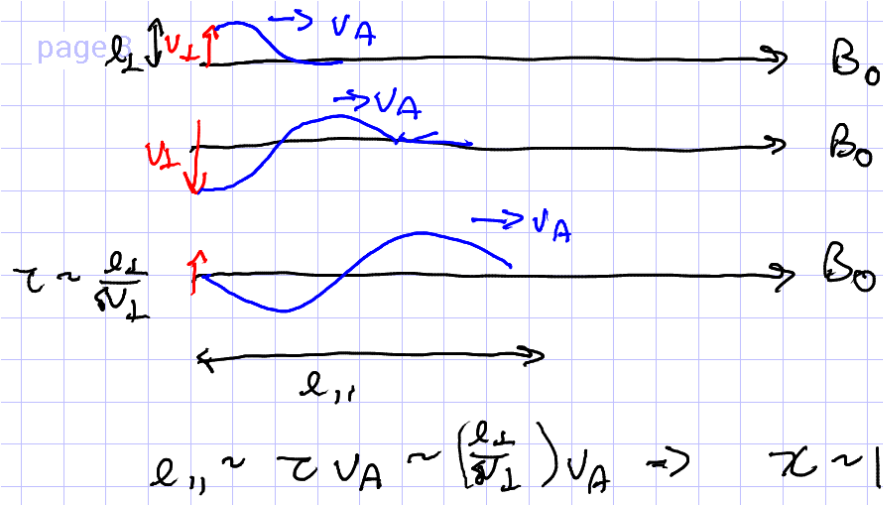


This requires that $l_{\parallel 1} \leq \tau_{\text{Eddy}} v_A$, or $\chi \leq 1$. So, these uncorrelated "eddies" upscale toward the $\chi=1$ line.

Related to this explanation is a simple physical argument in favor of critical balance.

Consider launching an Alfvén wave along B_0 by shaking the field line

page 3



Does everyone on the community believe in critical balance and the above interpretation? No!

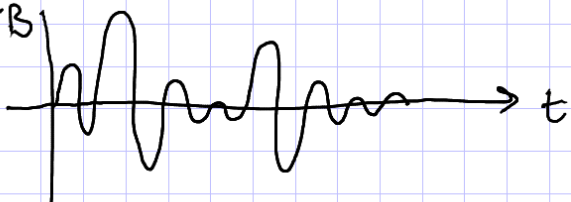
The interpretation of the fluctuations with $\chi > 1$ and the importance of $\chi \sim 1$ are mostly debated topics.

First, the importance of $\chi \sim 1$: While everyone agrees that $\chi \ll 1$ is described by linear wave dominated weak turbulence, what happens as $\chi \rightarrow 1$ is not agreed upon. As I drew in figure 1, which is supported by simulation but more on that shortly, most of the energy lies below the $\chi \sim 1$ line. Because of this, some believe that $\chi \sim 1$ is not that important and that turbulence is dominated by $\chi \gg 1$ fluctuations. So, they see plasma turbulence as being very similar to hydro turbulence; i.e., wave physics is minimally important and the fluctuations are primarily quasi-2D, eddy-like structures. Considerable evidence from simulations and solar wind measurements suggest linear wave modes play some role in turbulence, but what that role is and how they actively participate in the turbulence is unknown. Similarly, the importance and interpretation of the $\chi \gg 1$ fluctuations is very difficult to show convincingly. For instance, they could be as χ just

page 4 described them, or they could be an inevitable consequence of GS style turbulence for the reason outlined at the beginning of the lecture, i.e., they are 2D like eddies but rapidly cascade back to $\chi \approx 1$.

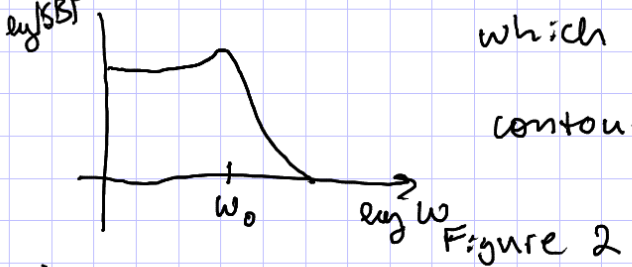
Two other interpretations:

1) If you consider a scale k_1^* in the middle of the inertial range, such a scale is always receiving energy from scales $k_1^{>*} > k_1^*$ and giving energy to scales $k_1^{<*} < k_1^*$. So, an Alfvén wave at that scale is constantly changing in amplitude, e.g. δB



$w_0 = k_1 v_A$, but the Fourier transform of this mode is which is very similar to the energy

contours on Figure 1.



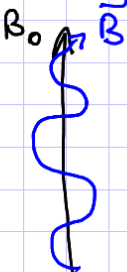
2) Some portion of the energy at $\chi \gg 1$ must be occupied by $k_{\parallel} \approx 0$ modes. As one enters strong turbulence, the wave matching condition becomes less restrictive because all orders contribute equally. So, k_{\parallel} need not be exactly zero. How far from zero it might extend will be covered later.

So, there is moderate disagreement about the meaning and interpretation of critical balance. Another major source of the disagreement stems from the meaning of k_z versus k_{\parallel} ...

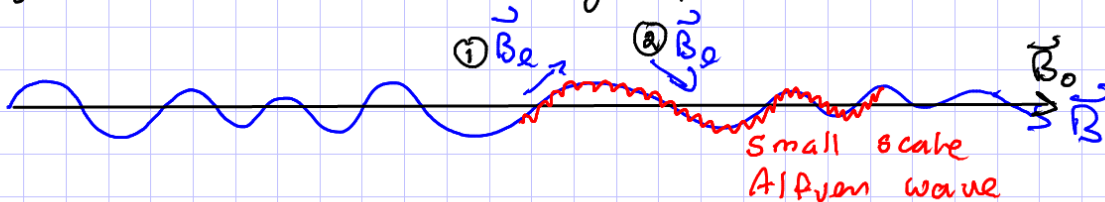
page 5 Local vs Global Wave Vector Anisotropy

The basic question we need to ask ourselves at this point is should we look for wavevector anisotropy along B_0 or along the local magnetic field?

Well, if we have a guide field B_0 with Alfvén waves (AWs) satisfying $\delta B_1 \sim B_0$, the total field, $\vec{B} = \vec{B}_0 + \vec{\delta B}$, may look like this

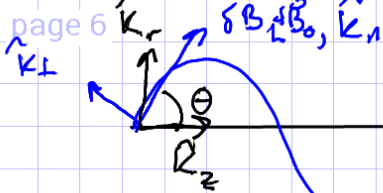


Smaller scale Alfvén waves propagate along the total field, not along the guide field. This can be seen by transforming to a Lagrangian reference frame, where it becomes clear that AWs move along the perturbed \vec{B} to lowest order. So, we might have the following picture



Note that at positions ① and ②, the small scale AW "sees" a guide field pointing in different directions, \vec{B}_{e1} and \vec{B}_{e2} . This also suggests that we don't need a uniform, constant guide field, B_0 , to consider GS type turbulence at small scales because a mean, more slowly varying, and larger scale field can serve as a local guide field for smaller scales. This is precisely the case in the solar wind, where the auto correlation length averaged field defines B_0 .

What does all of this mean in terms of determining the wavevector anisotropy of the turbulence?



$$\text{then } \Theta \approx \frac{\delta B_L}{B_0}$$

and δB_L is the RMS δB at the outer-scale, L ,

$$\text{and } k_z = -k_{\perp} \sin \theta + k_{\parallel} \cos \theta \quad \text{and} \quad k_r = k_{\perp} \cos \theta + k_{\parallel} \sin \theta$$

$$\therefore k_r \approx k_{\perp} + k_{\parallel} \Theta \quad \text{and} \quad k_z \approx k_{\perp} + k_{\parallel} \Theta$$

but $k_{\perp} \ll k_{\parallel}$ at small scales

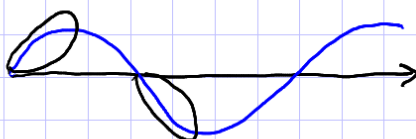
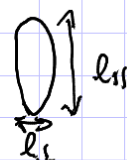
$$\Rightarrow k_r \approx k_{\perp} [1 + \Theta(\Theta^2)] \quad \text{and} \quad k_z \approx k_{\perp} \Theta \approx \frac{\delta B_L}{B_0} k_{\perp}$$

Thus, measuring \vec{k} with respect to B_0 will yield k_r and k_z , where $k_r \approx k_{\perp}$ and $k_z \approx \frac{\delta B_L}{B_0} k_{\perp}$. So, measuring wrt B_0 will give an accurate estimate of k_{\perp} , but k_z measures k_{\perp} again scaled by the outer-scale fluctuation amplitude.

In other words, the global anisotropy is set by $\frac{\delta B_L}{B_0}$.

The consequence of this is that a conventional FFT does the following to the anisotropy:

Consider a small-scale eddy of anisotropy



A FFT integrates over all orientations of

the eddy, which leads to the following anisotropy

~~for $\int k_r dk_r$~~ This is clearly distorted with respect to the original eddy, and the anisotropy is proportional to the field line wandering, i.e., $\frac{\delta B_L}{B_0}$.

All of the above suggests that we should measure wavevector anisotropy wrt the local magnetic field. Worse, it shows that measuring \vec{k} accurately requires a local measurement, and an accurate measurement of \vec{k} is necessary to test the validity of the critical balance conjecture.

page 7 Mesuring Local Anisotropy

The conceptually simplest method to measure $F(k_\parallel)$ and $F(k_\perp)$ is to sample along the total field and Fourier transform that signal. This obviously works because the sample at every point is along the local field, but it's computationally expensive and impossible on the solar wind.

The standard way to measure the local anisotropy was established by Cho & Vishniac (2000) and Narayan & Goldreich (2001):

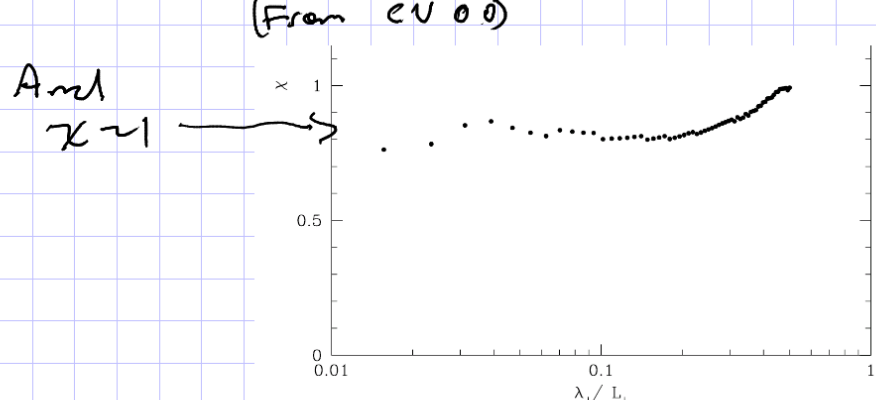
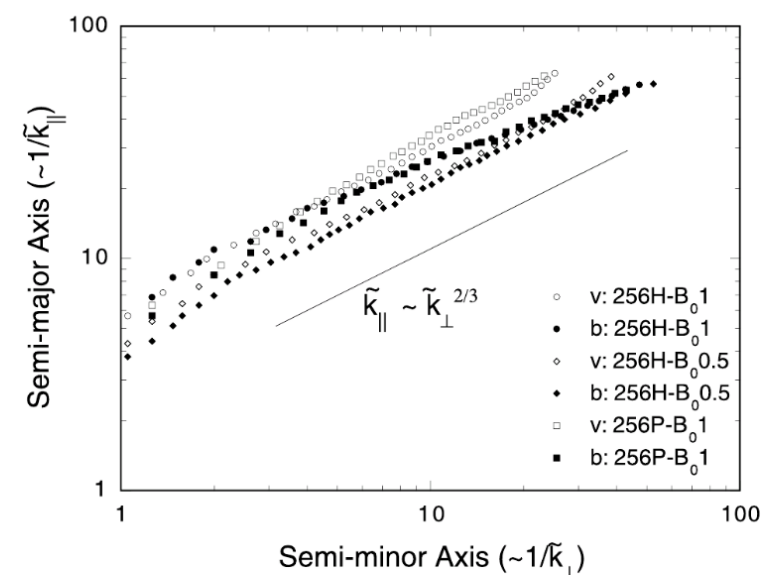
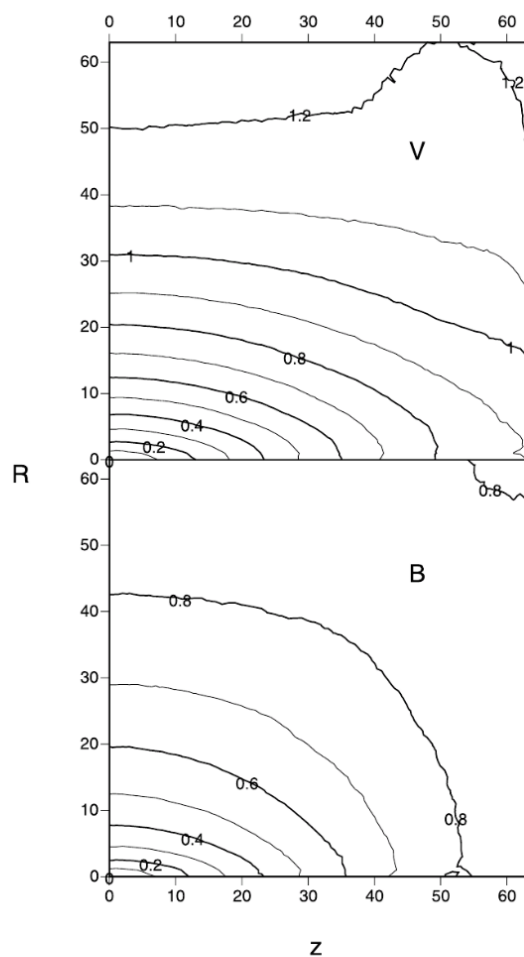
Rather than using a typical dual order dipole structure function in global coordinates $S(r, z) = \langle |B(r_1) - B(r_2)|^2 \rangle$ where $\hat{z} = \hat{b}_0$ and $\hat{r} = \hat{z} \times (\hat{r}_2 - \hat{r}_1)$ we could use

$$S_e(r, z) = \langle |B(r_1) - B(r_2)|^2 \rangle, \text{ where } \hat{z} = \frac{\vec{B}_e}{|\vec{B}_e|}, r = |\hat{z} \times (\hat{r}_2 - \hat{r}_1)|,$$

$$z = \hat{z} \cdot (\hat{r}_2 - \hat{r}_1) \text{ and } \vec{B}_e = (\vec{B}(r_1) + \vec{B}(r_2))/2. \text{ This approach yields}$$

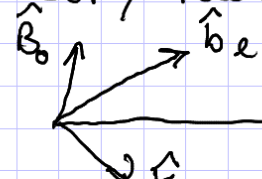
elongated eddies that grow with scale

$$k_n \propto k_\perp^{2/3}$$



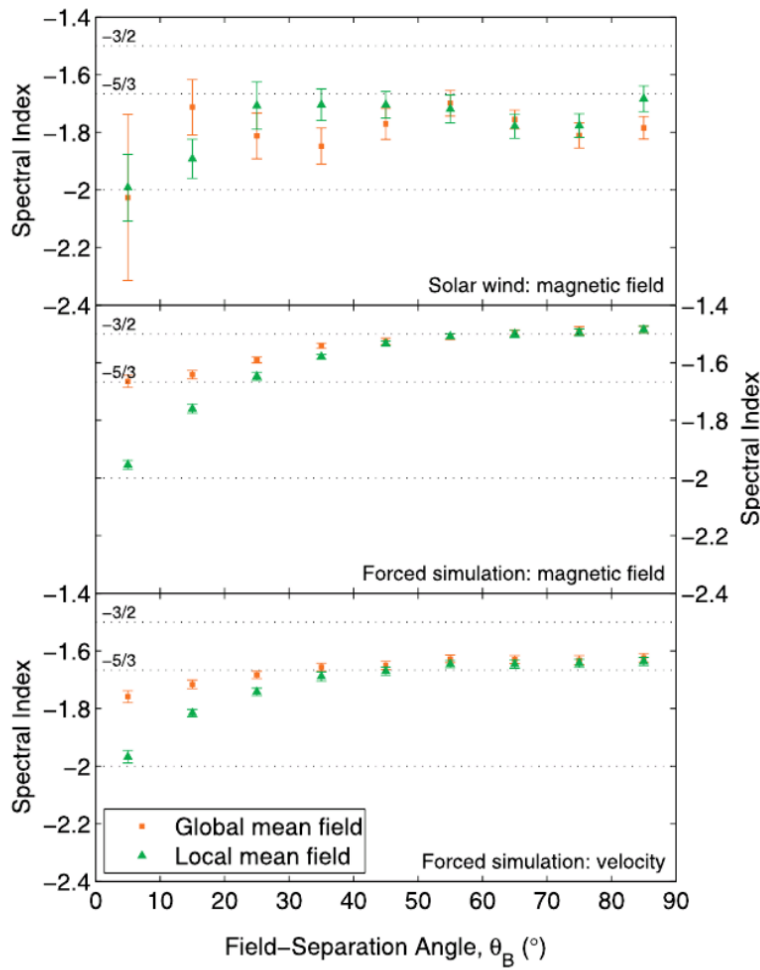
page 8 A similar approach is often used in the solar wind, but the measurement is trickier. In the solar wind, the solar wind speed at 1AU (earth) is $v_{sw} \approx 450 \frac{\text{km}}{\text{s}}$ and almost purely radial. So, a stationary (or quasi-stationary) spacecraft measures a Doppler shifted frequency as the plasma is advected past it

$w_{sc} = w_p + \vec{k} \cdot \vec{v}_{sw}$, where w_{sc} = spacecraft frame frequency and w_p = rest-frame plasma frequency. Since $v_{sw} \gg v_A, v_{ci}$ which are both $\sim 50 \frac{\text{km}}{\text{s}}$, Taylor's hypothesis is involved $w_p \ll \vec{k} \cdot \vec{v}_{sw} \Rightarrow w_{sc} \approx \vec{k} \cdot \vec{v}_{sw}$. So, the spacecraft frame frequency is equivalent to measuring spectral structure in the \vec{v}_{sw} direction. ∴, the measured \vec{k}_{sc} is not directly related to the field direction, either local or global



So, the spacecraft measures a reduced spectrum of the total \vec{k}_p vector projected onto \vec{v}_{sw} , and both \vec{B}_0 and \vec{b}_e may change at every sampled point. Recall that \vec{B}_0 is defined as the average of \vec{B} over an auto-correlation time in the plasma ($\sim 30-60$ m in the solar wind). So, $k_{||}$ is only measured when \vec{b}_e is approximately along \vec{v}_{sw} , and since $k_n \ll k_{\perp}$, \vec{b}_e must be very nearly parallel to \vec{v}_{sw} . As you might guess, this is rare. So, to produce k_n and k_{\perp} spectra requires many 30-60m intervals with similar plasma parameters, e.g. β, n, v_{sw}, \dots , to get good statistics on $k_{||}$. When this was applied to 65-hr intervals of Cluster data and local and global calculations were compared, Chen et al (2011)

page 9 found that RMHD simulations and the solar wind



are consistent with

$$E(k_1) \sim k_1^{-5/3}$$

$$E(k_n) \sim k_n^{-2}$$

$$E_B(k_1) \sim k_1^{-3/2}$$

about that next time. Also,

$$E(k_n) \sim k_n^{-2}$$

and local B for the solar

wind, but the error bars

are much larger for the

global field. It is

possible to sometimes

recover the correct

k_{11} in the solar wind using the global field, because $\frac{\delta B_x}{B_0} \ll 1$ and $\Rightarrow \hat{B}_x \approx \hat{B}_0$ and \hat{B}_0 may stay orthogonal with \hat{v}_{sw} for long periods. Such events are rare, however. Most global measurements of the SW, e.g. Tessman et al (1999), find isotropic scaling.

So, it looks like GS style critical balance works pretty well using the local B ! But wait, didn't GS actually use $k_Z = k \cdot \hat{B}_0$ in their theory? Yes, they did. Subsequently, they made the same sets of arguments I made above for using the local field, but the actual formulation of the GS model is in terms of B_0 . Many see this as a major deficiency of the model. The same group of many also object to using local measurements

for the following reason:

The energy, $(\delta B)^2$, is a well defined, 2nd order statistical quantity that does not depend on the phase relationships between various modes of the system. So, randomizing the phases of a DNS before computing energy spectra should produce exactly the same energy. Performing such a randomization procedure on the phases but not magnitudes of Fourier components yields

From
Matiagaeus
et al (2012)

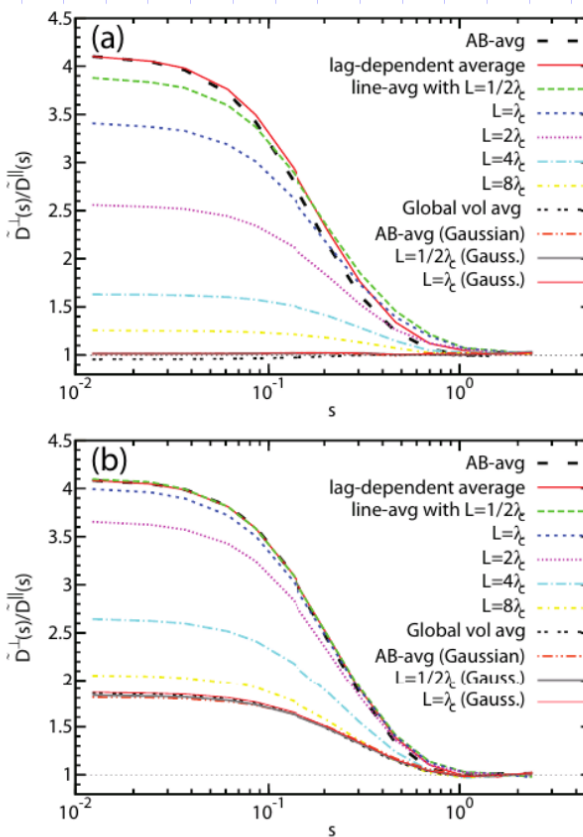


FIG. 1.— Anisotropy ratio $\tilde{D}^\perp(s)/\tilde{D}^\parallel(s)$ vs. lag s at inertial range and larger scales. Point and line average estimates of local mean field \mathbf{H} are used (“AB” averages the two points \mathbf{x}, \mathbf{x}' , “lag dependent” integrates from \mathbf{x} to \mathbf{x}' .) Perpendicular excitation is relatively enhanced, except for lags $s \gtrsim 1$ where isotropy holds (N.B. energy containing eddies are initially isotropic). (a) Results from $B_0 = 0$ simulation, with $\lambda_c = 0.34$ and $\lambda_{\text{diss}} = 0.021$. Anisotropy is stronger for more localized estimates of \mathbf{H} (e.g., shorter line averages). Randomizing phases (Gaussianizing – see text), produces isotropic results for all averaging methods and at all lags. Therefore, anisotropy is associated with non-Gaussian correlations. (b) Results from $B_0 = 1$ simulation, with $\lambda_c^\perp = 0.34$, $\lambda_c^\parallel = 0.43$, and $\lambda_{\text{diss}} = 0.022$. This case is anisotropic relative to the globally determined B_0 , and all methods based on local determinations of the mean field show further enhancement of anisotropy. For this run, phase randomization removes the enhanced local anisotropy, but global anisotropy remains.

The above is a valid objection to using the local field to measure the energy; however, the GS prediction requires the local field to estimate k_n rather than k_\parallel .

Clearly, the randomization decreases the measured local anisotropy but not the global. This means that measuring with the local \mathbf{B} necessarily folds higher order moments into the energy, because only moments above the second depend on phase. This is a consequence of using a stochastic coordinate system which is different at every point (or range of points).

page 11 Which is correct? I side with GS because there is a sound physical argument in favor of measuring wrt the local field, and even if the 2nd order, 2 point structure function conditioned on the local field direction is not actually a measurement of the energy but some mixed higher order quantity, I don't see how that actually matters or invalidates the GS predictions. But, I encourage you to decide for yourself.

Final Remark

those that are opposed to critical balance and the interpretation that linear wave physics is important state that the only evidence that will convince them that linear physics is important is a measured linear dispersion relationship. But, as figure 2 indicates, the recovery of a linear dispersion relationship in strong turbulence is not possible because the amplitude of any Fourier mode is modulated, leading to a broad range of frequencies at a given (k_x, k_y, k_z) rather than a delta function.

References

- 1) GS95: P. Goldreich & S. Sridhar ApJ 438, 763 (1995).
- 2) M601: J. Maron & P. Goldreich ApJ 554, 1175 (2001).
- 3) CVO: J. Cho & E. T. Vishniac ApJ 539, 273 (2000).
- 4) C. H. K. Chen et al MNRAS 415, 3219 (2011)
- 5) W. H. Matthaeus et al ApJ 750, 103 (2012)
- 6) J. A. Tasseon et al ApJ 692, 684 (2009).